

Sivers Asymmetry in Photoproduction of J/ψ and Jet at the EIC

Raj Kishore and Asmita Mukherjee

Department of Physics, Indian Institute of Technology Bombay, Powai, Mumbai 400076, India

Sangem Rajesh

Dipartimento di Fisica, Università di Cagliari, Cittadella Universitaria, I-09042 Monserrato (CA), Italy and

INFN, Sezione di Cagliari, Cittadella Universitaria, I-09042 Monserrato (CA), Italy

(Dated: February 21, 2020)

We calculate the Sivers asymmetry in the photoproduction of almost back-to-back J/ψ -jet pair in the process $ep^\uparrow \rightarrow J/\psi + \text{jet} + X$, which will be possible at the future planned electron-ion collider (EIC). We use the framework of generalized parton model (GPM), and NRQCD for calculating the J/ψ production rate. We include contributions from both color singlet and color octet states in the asymmetry. We obtain sizable Sivers asymmetry that can be promising to determine the gluon Sivers function. We also investigate the effect of TMD evolution on the asymmetry.

I. INTRODUCTION

Single spin asymmetries and transverse momentum dependent parton distributions (TMD pdfs) are objects of a lot of interest in recent days in hadron physics. Among the TMD pdfs Sivers function [1] is of particular interest. This gives the distribution of unpolarized quarks/gluons in a transversely polarized nucleon, which is not left-right symmetric with respect to the plane formed by the transverse momentum and spin of the nucleon. In some model calculations Sivers function is shown to be related to the quark orbital angular momentum through the GPD E_q [2]. Sivers function introduces an asymmetry, for example, in the azimuthal angle of the observed final state hadron in semi-inclusive deep inelastic scattering (SIDIS) and in the azimuthal angle correlations of the lepton pair in Drell-Yan process or back-to-back jets in pp collision, called the Sivers asymmetry. The first transverse moment of the Sivers function is related to the twist-three Qiu-Sterman function [3]. First experimental information on non-zero Sivers function for quarks was obtained from HERMES [4] and COMPASS [5] results. Since then, quite a lot of advances have been made, both in theory and experiment. Parametrization of quark Sivers function has been obtained in [6] and for gluons in [7, 8] by fitting data from RHIC within the DGLAP evolution approach. TMDs evolve with scale in a different way compared to the collinear pdfs. Much progress have been made in the past few years to understand the TMD evolution [9–11], and unpolarized distributions and fragmentation function have been calculated at NNLO [12]. A parametrization of the Sivers function incorporating the TMD evolution has been obtained in [13], however, gluon Sivers function (GSF) is not yet known. Therefore, compared to the quark TMDs, gluon TMDs are much less known, and these will also be investigated at the future electron-ion collider (EIC) [14] and the future fixed target plans at the LHC [15–17]. Gluon TMDs satisfy the positivity bounds first derived in [18]. A phenomenological bound on GSF was obtained [19], commonly known as Burkardt sum rule, from the requirement that the net transverse momentum of all partons (quarks and gluons) in a transversely polarized nucleon should vanish. In [20], a fit to the data from SIDIS at low scale indicates that this sum rule is almost saturated by contribution from u and d quarks, however, there may still be about 30% contribution from GSF.

Sivers function is a T-odd object and initial and final state interactions play an important role in Sivers asymmetry [21]. They are resummed into the gauge link or Wilson line in the operator definition of the Sivers function that is needed for color gauge invariance [22]. Gluon TMDs have two gauge links, in contrast to quark TMDs, that have only one. This introduces process dependence in them. The Sivers function in SIDIS is expected to be equal in magnitude but opposite in sign compared to the Sivers function appearing in the Drell-Yan process [21]. Recent data from RHIC [23] as well as COMPASS [24] seem to favour the sign change, however more data are needed [6]. The GSF for any process, in general can be written in terms of two independent functions, one of them has an operator structure that is C-even, and the other, C-odd. In the literature, the former is called a f-type Sivers function and the latter, d-type [25, 26]. In fact, one of these two (d-type) is not constrained by the Burkardt sum rule. More experimental data are needed to precisely determine the GSF. As is well known, J/ψ production in ep and pp collision is an effective method to probe the gluon TMDs including the GSF [27–33], as contribution to the Sivers asymmetry comes already at leading order (LO) through the virtual photon-gluon or gluon-gluon fusion processes, respectively. Data on Sivers asymmetry in J/ψ production are available from COMPASS collaboration [34], although with large error bars, it can be qualitatively explained by a LO calculation in NRQCD based color octet model [30]. In a recent work [35], maximal values of the azimuthal asymmetries in back-to-back electroproduction of J/ψ and a jet is estimated within the TMD factorization framework by neglecting the intrinsic transverse momentum of the initial parton in the hard part. Another interesting process to probe the GSF is quasi-real photoproduction of a hadron [36] or J/ψ [29, 37, 38].

Contribution to the single spin asymmetry (SSA) comes from J/ψ observed in the forward region that is when the transverse momentum (p_T) of J/ψ is small. In this work, we investigate the possibility to probe the GSF in quasi-real photoproduction of back-to-back J/ψ and jet by employing the generalized parton model (GPM) wherein the intrinsic transverse momentum of the initial parton is considered in the hard part, which will be possible in the future EIC. This will be sensitive to the GSF in a different kinematical region, and J/ψ observed need not be in the forward region.

As mentioned above, initial and final state interactions play a very important role in the SSAs. TMD factorization has been proven only for certain processes. The current status of the TMD factorization for heavy quarkonium production in pp collisions can be found in [39]. The most widely used approach to calculate amplitudes for J/ψ production is based on non-relativistic QCD (NRQCD). In this approach, the amplitude is factorized into a soft non-perturbative part and a hard part [40–46]. The heavy quark pair is produced in color singlet (CS) or color octet (CO) states in hard interaction. This is calculated in the perturbation theory. Then this heavy quark pair hadronizes to a quarkonium by emitting soft gluons. The hadronization process is described in terms of long distance matrix elements (LDMEs), that are obtained by fitting experimental data. The LDMEs have definite scaling properties with respect to the velocity parameter v , which is assumed to be small $v \ll 1$ [47]. The theoretical estimates are arranged in a double expansion in powers of v and the strong coupling, α_s . NRQCD has been successful in explaining hadroproduction data from TEVATRON [48, 49] and also J/ψ photoproduction data from HERA [50–53]. Both CS and CO contributions are needed to explain the HERA data [29]. In this work we calculate the weighted Sivers asymmetry, $A_N^{\sin(\phi_q)}$, in photoproduction of back-to-back J/ψ and jet at EIC in NRQCD by incorporating both CS and CO states. The plan of the paper is as follows. In section II we give the analytic expressions of the asymmetry. In section III we present the TMD evolution framework. Numerical results and conclusion are given in section IV and V respectively.

II. SIVERS ASYMMETRY

We consider the photoproduction process

$$e(l) + p^\uparrow(P) \rightarrow J/\psi(P_\psi) + \text{jet}(P_j) + X, \quad (1)$$

where the arrow in the superscript indicates the polarization of the proton. The letters in the round brackets represent the four momentum of the corresponding particles. We consider the proton-electron center of mass (C.M) frame wherein the proton and electron move along the $+z$ and $-z$ direction. The transverse plane, defined in FIG. 1, is orthogonal to the momentum of proton direction. The initial scattering electron radiates the virtual photon that will interact with the proton. The four momentum square of the virtual photon is $q^2 \approx -2E_e E'_e (1 - \cos \theta)$ with E_e and E'_e are energies of the initial and final scattered electron respectively. In the forward scattering limit, photoproduction, the four momentum of the virtual photon $q^2 = -Q^2 \rightarrow 0$ as a result the virtual photon becomes the real photon. The dominant subprocess for J/ψ production is the $\gamma(q) + g(p) \rightarrow J/\psi(P_\psi) + g(P_j)$ at next-to-leading order (NLO) in α_s . The quark (antiquark) initiated subprocess can also contribute $\gamma + q(\bar{q}) \rightarrow J/\psi + q(\bar{q})$. The unpolarized differential cross section for $ep \rightarrow J/\psi + \text{jet} + X$ process can be written as follows

$$E_\Psi E_j \frac{d\sigma}{d^3 \mathbf{P}_\Psi d^3 \mathbf{P}_j} = \frac{d\sigma}{d^2 \mathbf{P}_{\Psi\perp} dz d^2 \mathbf{P}_{j\perp} dz_1} = \frac{1}{4(2\pi)^2} \frac{1}{zz_1} \sum_a \int dx_\gamma dx_a d^2 \mathbf{p}_{a\perp} f_{\gamma/e}(x_\gamma) f_{a/p}(x_a, p_{a\perp}) \times \delta^4(q + p - P_\Psi - P_j) \frac{1}{2\hat{s}} |\mathcal{M}_{\gamma a \rightarrow J/\psi a}|^2, \quad (2)$$

where $a = g, u, d, s, \bar{u}, \bar{d}, \bar{s}$. The x_γ and x_a are the light-cone momentum fractions of photon and partons respectively, and $\mathbf{p}_{a\perp}$ is the transverse momentum of the initial parton. We have assumed TMD factorization in the GPM model with the inclusion of intrinsic transverse momentum of the initial parton in the hard part. When the exchanged photon is quasi-real, the interaction takes place through the Weizsäcker-Williams distribution function of the electron, $f_{\gamma/e}(x_\gamma)$, this describes the density of photons inside the electron and is given by [54]

$$f_{\gamma/e}(x_\gamma) = \frac{\alpha}{2\pi} \left[2m_e^2 x_\gamma \left(\frac{1}{Q_{min}^2} - \frac{1}{Q_{max}^2} \right) + \frac{1 + (1 - x_\gamma)^2}{x_\gamma} \ln \frac{Q_{max}^2}{Q_{min}^2} \right], \quad (3)$$

where α is the electromagnetic coupling and $Q_{min}^2 = m_e^2 \frac{x_\gamma^2}{1-x_\gamma}$, m_e being the electron mass. We have considered $Q_{max}^2 = 1 \text{ GeV}^2$ for estimating the Sivers asymmetry. The unpolarized TMD, $f_{a/p}$, represents the density of unpolarized partons inside an unpolarized proton with momentum fraction x_a and transverse momentum $p_{a\perp}$. The \hat{s} , \hat{t} and \hat{u} are

the Mandelstam variables at partonic level and their definitions are given in appendix A. $\mathcal{M}_{\gamma a \rightarrow J/\psi a}$ is the amplitude of gluon and quark (anti-quark) initiated subprocesses. The square of the amplitude is calculated using the NRQCD model, for more details Ref.[29] is referred for gluon channel, and the quark (anti-quark) channel matrix elements are given in the appendix B. The CS and CO states i.e., $^3S_1^{(1,8)}$, $^1S_0^{(8)}$ and $^3P_J^{(8)}$ are considered for J/ψ production. The center of mass (C.M) energy of the proton-electron system is $s = (P + l)^2$. In Eq.(2), the inelastic variables $z = \frac{P \cdot P_h}{P \cdot q}$ and $z_1 = \frac{P \cdot P_j}{P \cdot q}$ are the energy fractions transferred from photon to J/ψ and jet respectively in the proton rest frame. In photoproduction, the inelastic variables z and z_1 can be measured in experiments using the Jacquet-Blondel method [50, 51, 53]. By using the definitions of four momenta as given in appendix A, the momentum conservation delta function can be decomposed as

$$\delta^4(q + p - P_\Psi - P_j) = \frac{2}{x_\gamma s} \delta(1 - z - z_1) \delta\left(x_a - \frac{M^2 + P_{\Psi\perp}^2}{z x_\gamma s} - \frac{P_{j\perp}^2}{z_1 x_\gamma s}\right) \delta^2(\mathbf{p}_{a\perp} - \mathbf{P}_{\Psi\perp} - \mathbf{P}_{j\perp}), \quad (4)$$

where $\mathbf{P}_{\Psi\perp}$ and $\mathbf{P}_{j\perp}$ are the transverse momentum of the J/ψ and jet respectively and their azimuthal angles are represented with ϕ_1 and ϕ_2 such that $\delta\phi = \phi_2 - \phi_1 - \pi$ as shown in FIG. 1.

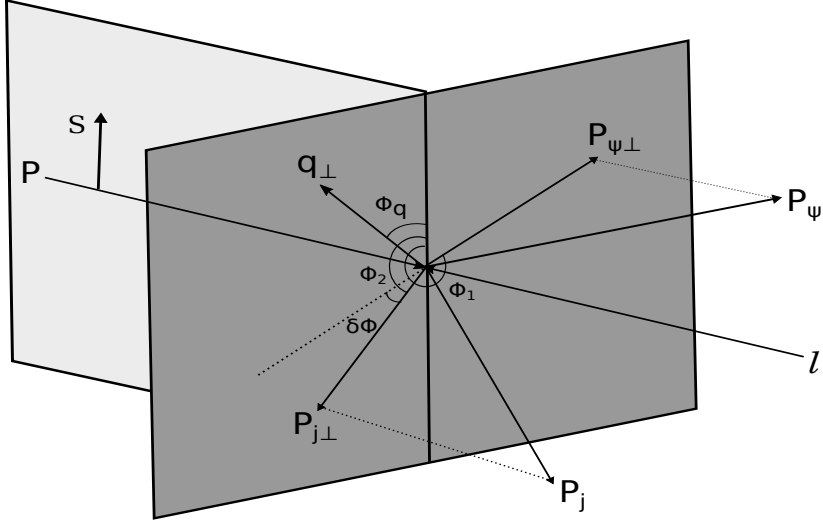


FIG. 1: Illustration of azimuthal angles in the $ep^\dagger \rightarrow J/\psi + \text{jet}$ process. The transverse momenta $\mathbf{P}_{\Psi\perp}$ and $\mathbf{P}_{j\perp}$ of J/ψ and jet respectively are in the plane orthogonal to the momentum of the proton P .

Now, we define the sum and difference of transverse momenta of J/ψ and jet as $\mathbf{q}_\perp = \mathbf{P}_{\Psi\perp} + \mathbf{P}_{j\perp}$ and $\mathbf{K}_\perp = (\mathbf{P}_{\Psi\perp} - \mathbf{P}_{j\perp})/2$. We are interested in the case where $|\mathbf{q}_\perp| \ll |\mathbf{K}_\perp|$ i.e., the J/ψ and jet are almost back to back in the transverse plane as shown in FIG. 1. The azimuthal angle of \mathbf{q}_\perp is denoted with ϕ_q . After integrating over z_1 , x_a and $\mathbf{p}_{a\perp}$, one obtain the following expression

$$\frac{d\sigma}{d^2\mathbf{q}_\perp dz d^2\mathbf{K}_\perp} = \frac{1}{2(2\pi)^2} \frac{1}{z(1-z)s} \sum_a \int \frac{dx_\gamma}{x_\gamma} f_{\gamma/e}(x_\gamma) f_{a/p}(x_a, q_\perp) \frac{1}{2\hat{s}} |\mathcal{M}_{\gamma a \rightarrow J/\psi a}|^2. \quad (5)$$

For a transversely polarized proton, the differential cross section is given by

$$\frac{d\sigma^{\uparrow(\downarrow)}}{d^2\mathbf{q}_\perp dz d^2\mathbf{K}_\perp} = \frac{1}{2(2\pi)^2} \frac{1}{z(1-z)s} \sum_a \int \frac{dx_\gamma}{x_\gamma} f_{\gamma/e}(x_\gamma) f_{a/p^{\uparrow(\downarrow)}}(x_a, q_\perp) \frac{1}{2\hat{s}} |\mathcal{M}_{\gamma a \rightarrow J/\psi a}|^2. \quad (6)$$

The weighted Siverts asymmetry is defined as [55]

$$A_N^{W(\phi_q)} \equiv \frac{\int d\phi_q W(\phi_q) (d\sigma^\uparrow - d\sigma^\downarrow)}{\int d\phi_q (d\sigma^\uparrow + d\sigma^\downarrow)} \equiv \frac{\int d\phi_q W(\phi_q) d\Delta\sigma(\phi_q)}{\int d\phi_q 2d\sigma}, \quad (7)$$

where $d\sigma^{\uparrow(\downarrow)}$ indicates the polarized cross section in the process where one of the initial particle is transversely polarized with respect to its momentum direction. The azimuthal weight factor $W(\phi_q) = -\sin(\phi_q)$ which is given by [56, 57]

$$-\sin(\phi_q) = \frac{(\mathbf{S} \times \hat{\mathbf{P}}) \cdot \mathbf{q}_\perp}{|\mathbf{S} \times \hat{\mathbf{P}}| |\hat{\mathbf{P}} \times \mathbf{q}_\perp|}. \quad (8)$$

It has been advertised that the J/ψ production probes the gluon TMDs and the quark contribution can be safely neglected in the kinematical region considered because of the insignificant contribution of quarks w.r.t gluon, which will be discussed in the results section. Hence the dominant contribution to the Sivers asymmetry comes from the gluon channel. The numerator of the asymmetry is sensitive to the Sivers function in J/ψ production

$$d\Delta\sigma \equiv \frac{d\sigma^\uparrow}{d^2\mathbf{q}_\perp dz d^2\mathbf{K}_\perp} - \frac{d\sigma^\downarrow}{d^2\mathbf{q}_\perp dz d^2\mathbf{K}_\perp} = \frac{1}{2(2\pi)^2} \frac{1}{z(1-z)_s} \sum_a \int \frac{dx_\gamma}{x_\gamma} f_{\gamma/e}(x_\gamma) \Delta \hat{f}_{a/p}(x_a, \mathbf{q}_\perp) \frac{1}{2\hat{s}} |\mathcal{M}_{\gamma a \rightarrow J/\psi a}|^2, \quad (9)$$

with $\Delta \hat{f}_{a/p^\uparrow}(x_a, \mathbf{q}_\perp)$ being the Sivers function, describes the number density of unpolarized partons in a transversely polarized proton with mass M_p . The analytic expressions for contributions from different states can be found in [29]. As only J/ψ was observed there, we had integrated over the phase space of the final gluon $a = g$, whereas here, the final parton is producing the observed jet. Sivers function in Trento convention [56] is given by

$$\begin{aligned} \Delta \hat{f}_{a/p^\uparrow}(x_a, \mathbf{q}_\perp) &\equiv \hat{f}_{a/p^\uparrow}(x_a, \mathbf{q}_\perp) - \hat{f}_{a/p^\downarrow}(x_a, \mathbf{q}_\perp) \\ &= \Delta^N f_{a/p^\uparrow}(x_a, q_\perp) \hat{\mathbf{S}} \cdot (\hat{\mathbf{P}} \times \hat{\mathbf{q}}_\perp) \\ &= -\Delta^N f_{a/p^\uparrow}(x_a, q_\perp) \sin(\phi_q) \\ &= -\frac{2}{M_p} f_{1T}^\perp(x_a, q_\perp) \hat{\mathbf{S}} \cdot (\hat{\mathbf{P}} \times \mathbf{q}_\perp). \end{aligned} \quad (10)$$

The Sivers function fulfills the following positivity bound

$$|\Delta^N f_{a/p^\uparrow}(x_a, q_\perp)| \leq 2 f_{a/p}(x_a, q_\perp), \quad \text{or} \quad \frac{q_\perp}{M_p} |f_{1T}^\perp(x_a, q_\perp)| \leq f_{a/p}(x_a, q_\perp). \quad (11)$$

Following Ref.[7, 8], we adopt the Gaussian parametrization for Sivers function within the DGLAP evolution approach as given below

$$\Delta^N f_{a/p^\uparrow}(x_a, q_\perp) = \left(-2 \frac{q_\perp}{M_p}\right) f_{1T}^\perp(x_a, q_\perp) = 2 \mathcal{N}_a(x_a) f_{a/p}(x_a) h(q_\perp) \frac{e^{-q_\perp^2/\langle q_\perp^2 \rangle}}{\pi \langle q_\perp^2 \rangle}, \quad (12)$$

where $f_{a/p}(x_a)$ is the usual collinear parton distribution function (PDF) which follows the DGLAP evolution equation and

$$\mathcal{N}_a(x_a) = N_a x_a^\alpha (1-x_a)^\beta \frac{(\alpha+\beta)^{(\alpha+\beta)}}{\alpha^\alpha \beta^\beta}, \quad (13)$$

with $|N_a| \leq 1$ and

$$h(q_\perp) = \sqrt{2e} \frac{q_\perp}{M'} e^{-q_\perp^2/M'^2}, \quad (14)$$

as a result the Sivers function satisfies the positivity bound for all values of x_a and q_\perp . If we define the parameter

$$\rho = \frac{M'^2}{\langle q_\perp^2 \rangle + M'^2}, \quad (15)$$

such that $0 < \rho < 1$, then Eq. (12) becomes

$$\Delta^N f_{a/p^\uparrow}(x_a, q_\perp) = 2 \frac{\sqrt{2e}}{\pi} \mathcal{N}_a(x_a) f_{a/p}(x_a) \sqrt{\frac{1-\rho}{\rho}} q_\perp \frac{e^{-q_\perp^2/\rho \langle q_\perp^2 \rangle}}{\langle q_\perp^2 \rangle^{3/2}}. \quad (16)$$

The unpolarized gluon TMD sitting in the denominator of the asymmetry is parametrized as Gaussian distribution

$$f_{a/p}(x_a, q_\perp) = \frac{1}{\pi \langle q_\perp^2 \rangle} f(x_a) e^{-q_\perp^2 / \langle q_\perp^2 \rangle}. \quad (17)$$

The best fit parameters of Siverson function have been extracted for quarks [6] and gluons [7, 8] from SIDIS and RHIC data respectively. In Ref. [8], new set of best fit parameters of GSF are extracted for $\langle q_\perp^2 \rangle = 1 \text{ GeV}^2$ and are tabulated in TABLE I.

Best fit parameters							
Evolution	a	N_a	α	β	ρ	$\langle q_\perp^2 \rangle \text{ GeV}^2$	Notation
DGLAP	g [7]	0.65	2.8	2.8	0.687	0.25	SIDIS1
	g [7]	0.05	0.8	1.4	0.576	0.25	SIDIS2
	g [8]	0.25	0.6	0.6	0.1	1.0	SIDIS3
TMD	u [13]	0.106	1.051	4.857		0.38	TMD-a
	d [13]	-0.163	1.552	4.857		0.38	TMD-b

TABLE I: Best fit parameters of Siverson function.

III. TMD EVOLUTION

In DGLAP evolution, collinear PDFs evolve with only the probing scale (μ). However, in TMD evolution approach, TMDs evolve with both the intrinsic transverse momentum ($p_{a\perp}$) of the parton and the probing scale. The TMD evolution framework is derived in the impact parameter space (b_\perp) [10]

$$f(x_a, b_\perp, \mu) = \int d^2 \mathbf{p}_{a\perp} e^{-i \mathbf{b}_\perp \cdot \mathbf{p}_{a\perp}} f(x_a, p_{a\perp}, \mu), \quad (18)$$

and in the momentum space is given by

$$f(x_a, p_{a\perp}, \mu) = \frac{1}{(2\pi)^2} \int d^2 \mathbf{b}_\perp e^{i \mathbf{b}_\perp \cdot \mathbf{p}_{a\perp}} f(x_a, b_\perp, \mu). \quad (19)$$

Usually, TMDs depend on two scales that are renormalization scale (μ) and auxiliary scale (ζ) [58, 59]. In order to cure the light-cone (rapidity) divergences in TMD factorization, the scale ζ has been introduced. One can obtain the renormalization group and Collins-Soper equations by taking scale evolution with respect to μ and ζ respectively. The unpolarized TMD expression at a given final scale $Q_f = \sqrt{\zeta} = M$ is obtained by solving RG and CS equations [13, 58, 59] and is given below

$$f(x_a, b_\perp, Q_f, \zeta) = f(x_a, b_\perp, Q_i) R_{pert}(Q_f, Q_i, b_*) R_{NP}(Q_f, b_\perp). \quad (20)$$

where $Q_i = c/b_*(b_\perp)$ is the initial scale of the TMD with $c = 2e^{-\gamma_\epsilon}$ and $\gamma_\epsilon \approx 0.577$. In line with Ref.[13], we adopt the b_* prescription to avoid hitting the Landau pole by freezing the scale b_\perp . Here, $b_*(b_\perp) = \frac{b_\perp}{\sqrt{1 + \left(\frac{b_\perp}{b_{\max}}\right)^2}} \approx b_{\max}$

when $b_\perp \rightarrow \infty$ and $b_*(b_\perp) \approx b_\perp$ when $b_\perp \rightarrow 0$. The R_{pert} and R_{NP} are the perturbative and the nonperturbative parts of the TMD respectively, which are given below

$$R_{pert}(Q_f, b_*) = \exp \left\{ - \int_{c/b_*}^{Q_f} \frac{d\mu}{\mu} \left(A \log \left(\frac{Q_f^2}{\mu^2} \right) + B \right) \right\}, \quad (21)$$

and

$$R_{NP}(Q_f, b_\perp) = \exp \left\{ - \left[g_1^{\text{TMD}} + \frac{g_2}{2} \log \frac{Q_f}{Q_0} \right] b_\perp^2 \right\}, \quad (22)$$

where the anomalous dimensions are $A = \sum_{n=1}^{\infty} \left(\frac{\alpha_s(\mu)}{\pi} \right)^n A_n$ and $B = \sum_{n=1}^{\infty} \left(\frac{\alpha_s(\mu)}{\pi} \right)^n B_n$, and the coefficients for gluon case are $A_1 = C_A$, $A_2 = \frac{1}{2} C_F \left(C_A \left(\frac{67}{18} - \frac{\pi^2}{6} \right) - \frac{5}{9} C_A N_f \right)$ and $B_1 = -\frac{1}{2} \left(\frac{11}{3} C_A - \frac{2}{3} N_f \right)$, and for quark case are

$A_1 = C_F$, $A_2 = \frac{1}{2}C_F \left(C_A \left(\frac{67}{18} - \frac{\pi^2}{6} \right) - \frac{5}{9}N_f \right)$ and $B_1 = -\frac{3}{2}C_F$ [13]. The unpolarized TMD at the initial scale can be written as

$$f(x_a, b_\perp, Q_i) = \sum_{i=g,q} \int_x^1 \frac{d\hat{x}}{\hat{x}} C_{i/a}(x_a/\hat{x}, b_\perp, \alpha_s, Q_i) f_{i/p}(\hat{x}, c/b_*) + \mathcal{O}(b_\perp \Lambda_{QCD}), \quad (23)$$

where $C_{i/a}$ is the perturbatively calculated process independent coefficient function, and is different for each type of TMD. The derivative of the Siverson function follows the same evolution equation as given in Eq.(20) but the g_1^{TMD} changes to g_1^{Sivers} in the R_{NP} factor. The Siverson function $f_{1T}^\perp(x_a, p_{a\perp}, Q_f)$ and it's derivative are related by Fourier transformation as below [59]

$$f_{1T}^\perp(x_a, p_{a\perp}, Q_f) = -\frac{1}{2\pi p_{a\perp}} \int_0^\infty db_\perp b_\perp J_1(p_{a\perp} b_\perp) f_{1T}^{\prime\perp}(x_a, b_\perp, Q_f), \quad (24)$$

and the unpolarized TMD is given by

$$f_{a/p}(x_a, p_{a\perp}, Q_f) = \frac{1}{2\pi} \int_0^\infty db_\perp b_\perp J_0(p_{a\perp} b_\perp) f_{a/p}(x_a, b_\perp, Q_f), \quad (25)$$

The derivative of the Siverson function at the initial scale Q_i can be written in terms of Qiu-Sterman function as below [22, 60]

$$f_{1T}^{\prime\perp}(x_a, b_\perp, Q_i) \simeq \frac{M_p b_\perp}{2} T_{a,F}(x_a, x_a, Q_i), \quad (26)$$

where $T_{a,F}(x_a, x_a, Q_i)$ is the Qiu-Sterman function, which is usually assumed to be proportional to collinear PDF [13, 61]

$$T_{a,F}(x_a, x_a, Q_i) = \mathcal{N}_a(x_a) f_{a/p}(x_a, Q_i), \quad (27)$$

the definition of $\mathcal{N}_a(x_a)$ is given in Eq.(13). Note that here we have used the fact that Siverson function in Drell-Yan process have opposite sign compared to the Siverson function in semi-inclusive DIS. So far the best fit parameters of GSF have not been extracted in the TMD evolution approach. However only the u and d quark Siverson function are known which were extracted in [13] from SIDIS data within TMD evolution scheme, which are tabulated in TABLE I. As so far a fit for the gluon Siverson function is not available in the TMD evolution approach, in order to show the effect of this evolution on the asymmetry, we use an exploratory approach, namely, following Ref.[62], we define the following two set of parametrizations for GSF by using the known u and d quark Siverson function parameters

$$\begin{aligned} (a) \quad \mathcal{N}_g(x_g) &= (\mathcal{N}_u(x_g) + \mathcal{N}_d(x_g))/2 \\ (b) \quad \mathcal{N}_g(x_g) &= \mathcal{N}_d(x_g). \end{aligned} \quad (28)$$

We denote the first parametrization as TMD-a and second one as TMD-b. As the sign of N_u and N_d are opposite, TMD-a gives a small GSF and TMD-b gives a large GSF. As mentioned in the introduction, Burkardt sum rule [19] gives a constraint on the GSF. However, in order to implement the constraint from the Burkardt sum rule contribution from all quark favours need to be included, and sea quark Siverson function is still not well constrained. Assuming contributions only from u and d quarks and gluons, we have checked that TMD-a parametrization satisfies the Burkardt sum rule, violation is about 1%; whereas the TMD-b parametrization violates the sum rule by about 19%. The numerical values of best fit parameters are estimated [13] at $Q_0 = \sqrt{2.4}$ GeV, $b_{\text{max}} = 1.5$ GeV⁻¹, $g_2 = 0.16$ GeV² and $\langle p_{s\perp}^2 \rangle = 0.282$ GeV² with $g_1^{\text{pdf}} = \langle p_{a\perp}^2 \rangle / 4 = \langle q_\perp^2 \rangle / 4$ and $g_1^{\text{sivers}} = \langle p_{s\perp}^2 \rangle / 4$. The numerator and denominator parts of Eq.(7) in TMD evolution approach can be written as the following

$$d\Delta\sigma = -\frac{1}{\pi M_p} \frac{1}{2(2\pi)^2} \frac{1}{z(1-z)s} \sum_a \int \frac{dx_\gamma}{x_\gamma} db_\perp b_\perp J_1(q_\perp b_\perp) f_{1T}^{\prime\perp}(x_a, b_\perp, Q_f) f_{\gamma/e}(x_\gamma) \frac{1}{2\delta} |\mathcal{M}_{\gamma a \rightarrow J/\psi a}|^2 \sin(\phi_q), \quad (29)$$

$$2d\sigma = \frac{1}{2(2\pi)^2} \frac{1}{\pi z(1-z)s} \sum_a \int \frac{dx_\gamma}{x_\gamma} db_\perp b_\perp J_0(q_\perp b_\perp) f_{a/p}(x_a, b_\perp, Q_f) f_{\gamma/e}(x_\gamma) \frac{1}{2\delta} |\mathcal{M}_{\gamma a \rightarrow J/\psi a}|^2. \quad (30)$$

IV. NUMERICAL RESULTS

In this section, we discuss the numerical results of Siverson asymmetry in $ep^\dagger \rightarrow J/\psi + \text{jet} + X$ photoproduction process, where the proton is transversely polarized. We consider the situation $|\mathbf{q}_\perp| \ll |\mathbf{K}_\perp|$ i.e., the produced pair of J/ψ and jet are almost back to back in the transverse plane as shown in FIG. 1. This configuration is feasible in the future proposed Electron-Ion collider (EIC) with C.M energy from 20 to 150 GeV. The NLO photon-gluon fusion and quark (anti-quark) initiated subprocesses, $\gamma g \rightarrow J/\psi g$ and $\gamma q(\text{ or } \bar{q}) \rightarrow J/\psi q(\text{ or } \bar{q})$, are considered. The NRQCD model is employed for J/ψ production, and the CS and CO states are considered for both numerator and denominator parts of Eq.(7). If we do not detect the jet in the final state then CS state does not contribute to the asymmetry, because the initial and final state interactions between the final state parton and remnant of the proton get canceled with each other as discussed in [63]. The values of long distance matrix elements (LDMEs) are taken from Ref.[64]. There are different set of LDMEs in the literature and the asymmetry is found to be independent of the choice of LDME set.

There are two types of J/ψ photoproductions that are resolved and direct photon contributions. The resolved photoproduction, the photon splits into partons which subsequently interact with the partons of proton, contributes to J/ψ production in the low z region ($z < 0.3$). While in the direct photoproduction, the photon directly interacts electromagnetically with the partons from the proton. For direct inelastic J/ψ photoproduction one has to consider $0.3 < z < 0.9$ as discussed in Ref.[29]. The fragmentation of gluon and heavy quark can also contribute to J/ψ production at high transverse momentum of the J/ψ [65]. The feed-down contribution from an excited state $\psi(2S)$ and the decay of χ_c states contribution to J/ψ are 15% [52] and 1% [66, 67] respectively, are not considered in this work. The final state parton becomes soft at $z \rightarrow 1$ which leads to infrared singularity. Therefore, to calculate the asymmetry for direct inelastic J/ψ photoproduction we consider $z = 0.3$. The mass of J/ψ is taken to be $M = 3.1$ GeV. The cteq611 PDF sets are used for collinear PDFs [68].

The Siverson asymmetry is calculated at EIC for $\sqrt{s} = 45$ and 100 GeV within the DGLAP and TMD evolution approaches. In DGLAP evolution approach, the GSF has been extracted in [7] from pion data at RHIC for fixed Gaussian width $\langle q_\perp^2 \rangle = 0.25$ GeV². Recently refitted the RHIC data with new set of GSF parameters for $\langle q_\perp^2 \rangle = 1$ GeV² [8]. However, GSF has not been extracted yet in TMD evolution approach. The u and d quark Siverson functions are extracted in Ref.[13] using TMD evolution approach. For numerical estimation of Siverson asymmetry, the u and d quark Siverson function best fit parameters are used for GSF as defined in Eq.(28) within TMD evolution approach. The best fit parameters of GSF and quark Siverson function are tabulated in TABLE I. The convention of figures as follows. The obtained Siverson asymmetry in DGLAP approach is represented with SIDIS1, SIDIS2 and SIDIS3. The TMD-a and TMD-b represent the Siverson asymmetry in TMD evolution approach.

In FIG. 2 - 4, the asymmetry in DGLAP and TMD evolution approaches as a function of q_\perp is shown at $\sqrt{s} = 45$ and 100 GeV for $K_\perp = 3$ GeV respectively at $z = 0.3$. The asymmetry is shown in the range $0 \leq q_\perp \leq 1$ GeV which is considered to satisfy the condition $|\mathbf{q}_\perp| \ll |\mathbf{K}_\perp|$. The value of $K_\perp = 3$ GeV is chosen of the order of J/ψ mass. For higher values of K_\perp and z the gluon channel contribution is suppressed because the momentum fraction of the parton, x_a , depends quadratically on K_\perp which can be seen from Eq.(4).

The maximized Siverson asymmetry, A_N^{Max} , at $\sqrt{s} = 45$ GeV is shown in FIG.2. Here, we saturated the Siverson function bound by adopting $\mathcal{N}_a = 1$ and $\rho = 2/3$ [8] in the parametrization of Siverson function which is given in Eq.(12). In the left panel of FIG.2, the gluon and quark (antiquark) channels contribution to A_N^{Max} is shown, and the quark (antiquark) channel contribution is insignificant compared to gluon channel. On this basis we can say that the pair of J/ψ +jet photoproduction process is an effective channel that probes the poorly known GSF in the kinematical region considered here. We have neglected the quark channel contribution to the numerator part of the asymmetry in FIG. 3 - 4. In the right panel of FIG.2, the individual CS and CO states contribution to A_N^{Max} is shown. The $^3S_1^{(1)}$ and $^1S_0^{(8)}$ states contribute largely to A_N^{Max} which is independent of \sqrt{s} .

In the left panel of FIG. 3, the weighted Siverson asymmetry, $A_N^{\sin(\phi_q)}$, is estimated to be about 3%, 1% and 6% respectively for SIDIS1, SIDIS2 and SIDIS3 set of GSF parameters at $\sqrt{s} = 45$ GeV. The $A_N^{\sin(\phi_q)}$ is reduced about 2% for $\sqrt{s} = 100$ GeV as shown in the right panel of FIG. 3. In FIG. 4, negative Siverson asymmetry is shown in TMD evolution approach. The sign of the Siverson asymmetry depends on relative magnitude of N_u and N_d and these have opposite sign which can be observed in TABLE I. For TMD-b parameter set, the \mathcal{N}_g is assumed to be proportional to \mathcal{N}_d of d quark, see the Eq.(28). The values of N_d is negative which leads to negative asymmetry. The average of u and d quarks x_a -dependent factor, \mathcal{N}_a , is defined for gluon as given in Eq.(28) for TMD-a parameter set. The magnitude of \mathcal{N}_d is comparable but slightly dominant compared to \mathcal{N}_u that leads to negative and small asymmetry for TMD-a parameter set. In FIG. 4, $A_N^{\sin(\phi_q)}$ is estimated maximum of 8% and 4% at $\sqrt{s} = 45$ and 100 GeV for TMD-b parameter set.

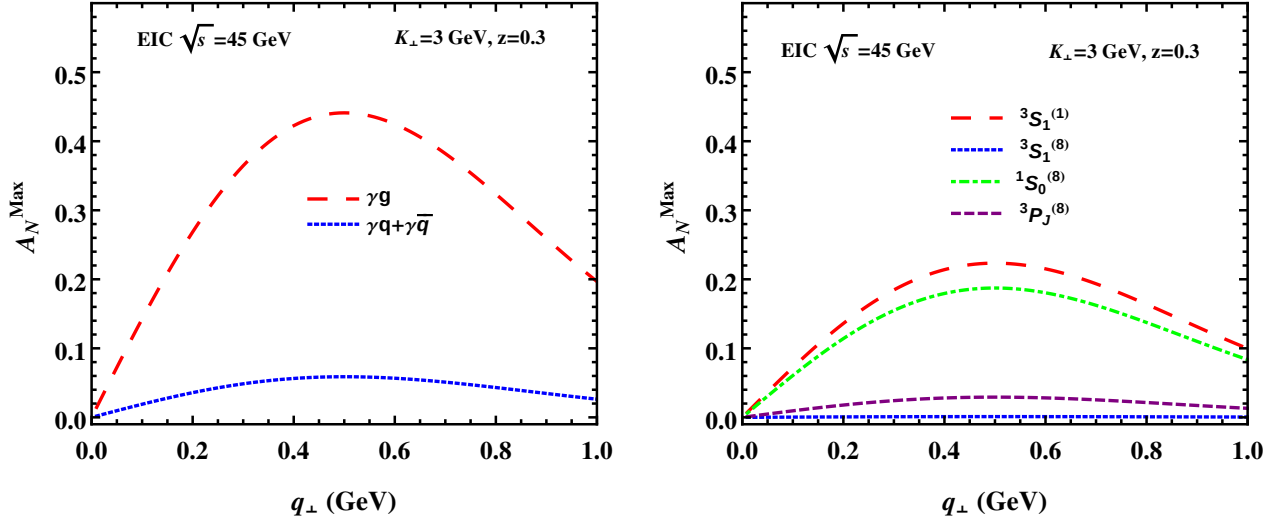


FIG. 2: (color online) Maximized Siverson asymmetry in $e + p^\dagger \rightarrow J/\psi + \text{jet} + X$ process as a function of q_\perp at EIC $\sqrt{s} = 45$ GeV. The Siverson function is saturated by adopting $\mathcal{N}_g(x) = 1$ and $\rho = 2/3$ for the parametrization of Siverson function given in Eq.(16). Left panel: for gluon and quark (antiquark) initiated subprocesses contribution to the asymmetry. Right panel: for different CS and CO states contribution to the maximum asymmetry.

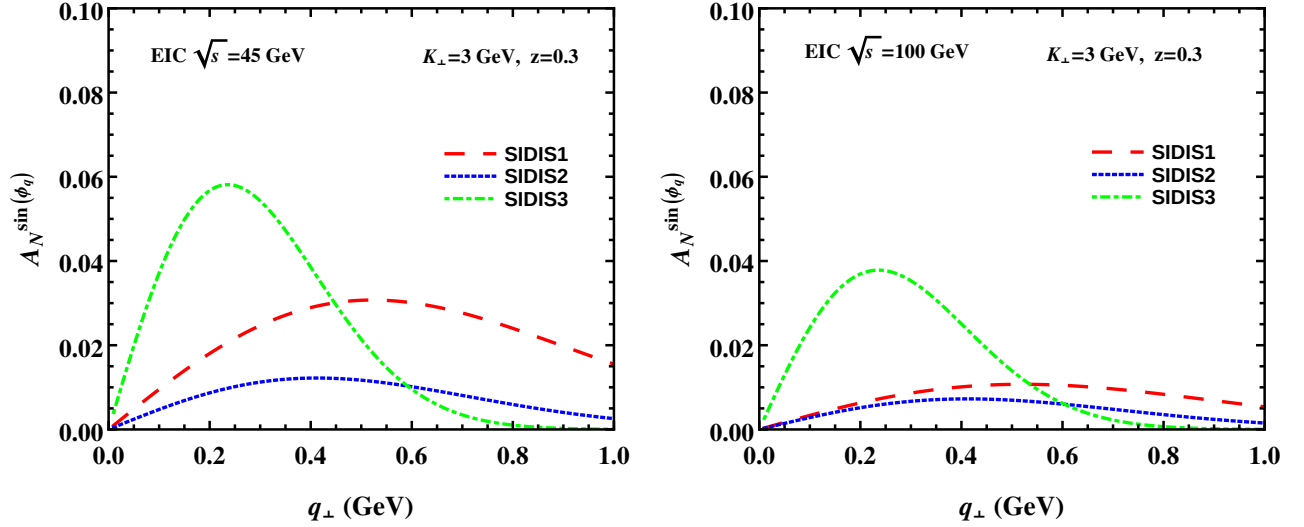


FIG. 3: (color online) The weighted Siverson asymmetry in $e + p^\dagger \rightarrow J/\psi + \text{jet} + X$ process as a function of q_\perp at EIC (a) $\sqrt{s} = 45$ GeV (left panel) and (b) $\sqrt{s} = 100$ GeV (right panel) using DGLAP evolution approach for SIDIS1, SIDIS2 and SIDIS3 GSF parametrization sets which are given in TABLE I.

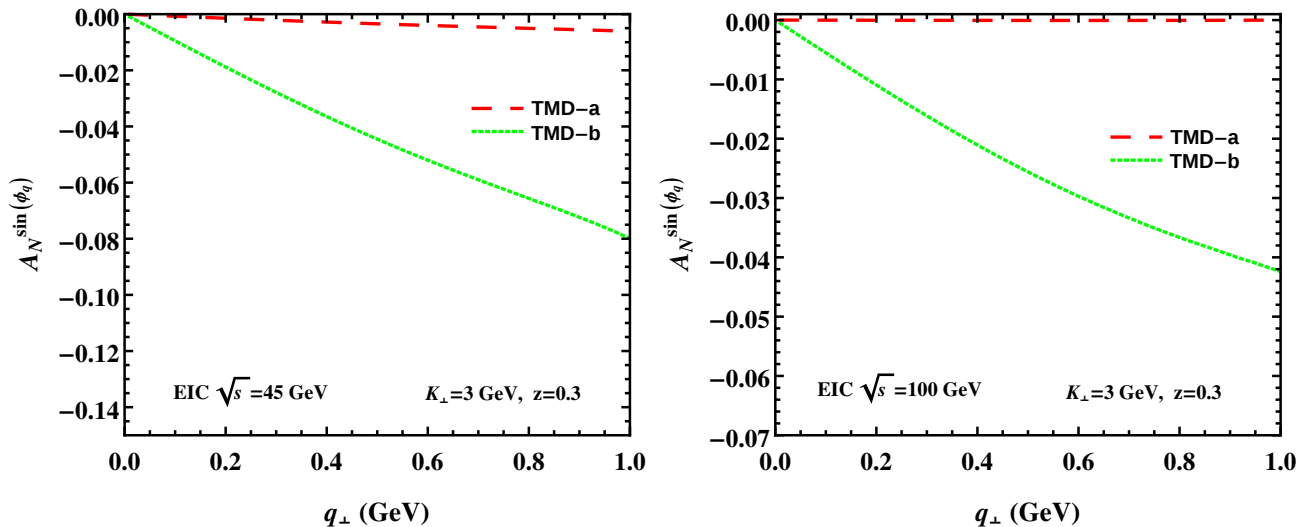


FIG. 4: (color online) The weighted Siverts asymmetry in $e + p^\dagger \rightarrow J/\psi + \text{jet} + X$ process as a function of q_\perp at EIC (a) $\sqrt{s} = 45$ GeV (left panel) and (b) $\sqrt{s} = 100$ GeV (right panel) using TMD evolution approach for TMD-a and TMD-b GSF parametrization sets which are given in TABLE I.

V. CONCLUSION

In this work, we gave an estimate of the Siverts asymmetry in almost back-to-back J/ψ and jet photoproduction at the future EIC. We assumed TMD factorization for this process and used generalized parton model, incorporating the intrinsic transverse momenta. The quasi-real photoproduction takes place through the Weizsäcker-Williams photon distribution of the electron. We used NRQCD to calculate the J/ψ production and incorporated both CS and CO contributions to the asymmetry. Major contribution comes from $^3S_1^{(1)}$ and $^1S_0^{(8)}$ states. We have also shown the effect of the TMD evolution on the asymmetry. In fact the Siverts asymmetry is positive without incorporating the TMD evolution, whereas it becomes negative when evolution is incorporated. We have obtained sizable Siverts asymmetry where the main contribution comes from the gluon Siverts function and the quark contribution is small. Therefore, back-to-back production of J/ψ and jet at the future EIC is a promising tool to access the gluon Siverts function.

Acknowledgment

We would like to thank Cristian Pisano and Pieter Taelis for useful discussions. The work of S.R. is supported by Fondazione Sardegna under the project Quarkonium at LHC energies, CUP F71I17000160002 (University of Cagliari). A.M. would like to thank University of Cagliari and INFN, Cagliari, Italy for hospitality where the final stage of this work was completed.

Appendices

Appendix A: Kinematics

We consider the frame in which the proton and electron are moving along $+z$ and $-z$ -axes respectively and their four momenta are given by

$$P = \frac{\sqrt{s}}{2}(1, 0, 0, 1), \quad l = \frac{\sqrt{s}}{2}(1, 0, 0, -1). \quad (\text{A1})$$

The C.M energy of electron-proton system is $s = (P + l)^2$. The above four momenta in light-cone coordinate system can be written as

$$P^\mu = \sqrt{\frac{s}{2}} n_+^\mu, \quad l^\mu = \sqrt{\frac{s}{2}} n_-^\mu, \quad (\text{A2})$$

where n_+ and n_- are two light-like vectors with $n_+ \cdot n_- = 1$ and $n_+^2 = n_-^2 = 0$.

$$n_+^\mu = (1, 0, \mathbf{0}), \quad n_-^\mu = (0, 1, \mathbf{0}). \quad (\text{A3})$$

We assume that the quasi-real photon is collinear to the electron. The quasi-real photon and parton four momenta are given by

$$q^\mu = x_\gamma \sqrt{\frac{s}{2}} n_-^\mu, \quad (\text{A4})$$

$$p = \frac{P_{\perp a}^2}{2x_a \sqrt{\frac{s}{2}}} n_-^\mu + x_a \sqrt{\frac{s}{2}} n_+^\mu + \mathbf{P}_{\perp a}^\mu \approx x_a \sqrt{\frac{s}{2}} n_+^\mu + \mathbf{P}_{\perp a}^\mu, \quad (\text{A5})$$

where $x_\gamma = \frac{q^-}{l^-}$ and $x_a = \frac{p^+}{P^+}$ are the light-cone momentum fractions. The four momentum of the J/ψ and final parton are given by

$$P_\Psi^\mu = zx_\gamma \sqrt{\frac{s}{2}} n_-^\mu + \frac{M^2 + P_{\Psi\perp}^2}{2zx_\gamma \sqrt{\frac{s}{2}}} n_+^\mu + \mathbf{P}_{\Psi\perp}^\mu. \quad (\text{A6})$$

$$P_j^\mu = z_1 x_\gamma \sqrt{\frac{s}{2}} n_-^\mu + \frac{P_{j\perp}^2}{2z_1 x_\gamma \sqrt{\frac{s}{2}}} n_+^\mu + \mathbf{P}_{j\perp}^\mu. \quad (\text{A7})$$

The inelastic variables are defined as $z = \frac{P \cdot P_\Psi}{P \cdot q} = \frac{P_\Psi^-}{q^-}$ and $z_1 = \frac{P \cdot P_j}{P \cdot q} = \frac{P_j^-}{q^-}$. By using the above relations, we can write down the expressions of Mandelstam variables as below

$$\hat{s} = (q + p)^2 = 2k \cdot q = sx_a x_\gamma, \quad (\text{A8})$$

$$\hat{t} = (q - P_j)^2 = -2q \cdot P_j = -\frac{P_{j\perp}^2}{z_1}, \quad (\text{A9})$$

$$\begin{aligned} \hat{u} &= (q - P_\Psi)^2 = M^2 - 2q \cdot P_\Psi \\ &= M^2 - \frac{M^2 + P_{\Psi\perp}^2}{z}. \end{aligned} \quad (\text{A10})$$

Here M being the mass of J/ψ .

Appendix B: Matrix elements for $\gamma + q(\bar{q}) \rightarrow J/\psi + q(\bar{q})$ subprocess

In this section the matrix elements for $\gamma + q(\bar{q}) \rightarrow J/\psi + q(\bar{q})$ channel are presented:

$$|\mathcal{M}(^3S_1^{(1)})|^2 = 0, \quad (\text{B1})$$

$$|\mathcal{M}(^3S_1^{(8)})|^2 = \frac{-2(4\pi)^3 e_c^2 \alpha_s^2 \alpha}{9M^3 \hat{s} \hat{t}} \langle 0 | \mathcal{O}_8^{J/\psi} (^3S_1) | 0 \rangle [\hat{s}^2 + \hat{t}^2 + 2\hat{u}M^2], \quad (\text{B2})$$

$$|\mathcal{M}(^1S_0^{(8)})|^2 = \frac{-4(4\pi)^3 e_c^2 \alpha_s^2 \alpha}{3M} \langle 0 | \mathcal{O}_8^{J/\psi} (^1S_0) | 0 \rangle \frac{\hat{s}^2 + \hat{t}^2}{\hat{u}(\hat{s} + \hat{t})^2}, \quad (\text{B3})$$

$$|\mathcal{M}(^3P_0^{(8)})|^2 = \frac{-16(4\pi)^3 e_c^2 \alpha_s^2 \alpha}{9M^3} \langle 0 | \mathcal{O}_8^{J/\psi} (^3P_0) | 0 \rangle \frac{(\hat{s}^2 + \hat{t}^2)(\hat{u} - 3M^2)^2}{\hat{u}(\hat{s} + \hat{t})^4}, \quad (\text{B4})$$

$$|\mathcal{M}(^3P_1^{(8)})|^2 = \frac{-32(4\pi)^3 e_c^2 \alpha_s^2 \alpha}{9M^3} \langle 0 | \mathcal{O}_8^{J/\psi} (^3P_1) | 0 \rangle \frac{(\hat{s}^2 + \hat{t}^2)\hat{u} + 4M^2\hat{s}\hat{t}}{(\hat{s} + \hat{t})^4}, \quad (\text{B5})$$

$$|\mathcal{M}(^3P_2^{(8)})|^2 = \frac{32(4\pi)^3 e_c^2 \alpha_s^2 \alpha}{45M^3 \hat{u}(\hat{s} + \hat{t})^4} \langle 0 | \mathcal{O}_8^{J/\psi} (^3P_2) | 0 \rangle \left[-\hat{u}^2 (7\hat{s}^2 + 12\hat{s}\hat{t} + 7\hat{t}^2) - 12\hat{u} (\hat{s}^2 + \hat{s}\hat{t} + \hat{t}^2) (\hat{s} + \hat{t}) - 6 (\hat{s}^2 + \hat{t}^2) (\hat{s} + \hat{t})^2 \right]. \quad (\text{B6})$$

The matrix elements for $\gamma g \rightarrow J/\psi + g$ channel are given in our previous paper [29].

-
- [1] D. W. Sivers, Phys. Rev. **D41**, 83 (1990).
[2] M. Burkardt, Nucl. Phys. **A735**, 185 (2004), hep-ph/0302144.
[3] J.-w. Qiu and G. F. Sterman, Phys. Rev. Lett. **67**, 2264 (1991).
[4] A. Airapetian et al. (HERMES), Phys. Rev. Lett. **94**, 012002 (2005), hep-ex/0408013.
[5] C. Adolph et al. (COMPASS), Phys. Lett. **B717**, 383 (2012), 1205.5122.
[6] M. Anselmino, M. Boglione, U. D'Alesio, F. Murgia, and A. Prokudin, JHEP **04**, 046 (2017), 1612.06413.
[7] U. D'Alesio, F. Murgia, and C. Pisano, JHEP **09**, 119 (2015), 1506.03078.
[8] U. D'Alesio, C. Flore, F. Murgia, C. Pisano, and P. Taels, Phys. Rev. **D99**, 036013 (2019), 1811.02970.
[9] S. M. Aybat, J. C. Collins, J.-W. Qiu, and T. C. Rogers, Phys. Rev. **D85**, 034043 (2012), 1110.6428.
[10] S. M. Aybat and T. C. Rogers, Phys. Rev. **D83**, 114042 (2011), 1101.5057.
[11] J. Collins and T. C. Rogers, Phys. Rev. **D96**, 054011 (2017), 1705.07167.
[12] M. G. Echevarria, I. Scimemi, and A. Vladimirov, JHEP **09**, 004 (2016), 1604.07869.
[13] M. G. Echevarria, A. Idilbi, Z.-B. Kang, and I. Vitev, Phys. Rev. **D89**, 074013 (2014), 1401.5078.
[14] A. Accardi et al., Eur. Phys. J. **A52**, 268 (2016), 1212.1701.
[15] S. J. Brodsky, F. Fleuret, C. Hadjidakis, and J. P. Lansberg, Phys. Rept. **522**, 239 (2013), 1202.6585.
[16] D. Kikoa, M. G. Echevarria, C. Hadjidakis, J.-P. Lansberg, C. Lorc, L. Massacrier, C. M. Quintans, A. Signori, and B. Trzeciak, Few Body Syst. **58**, 139 (2017), 1702.01546.
[17] B. Trzeciak, C. Da Silva, E. G. Ferreira, C. Hadjidakis, D. Kikola, J. P. Lansberg, L. Massacrier, J. Seixas, A. Uras, and Z. Yang, Few Body Syst. **58**, 148 (2017), 1703.03726.
[18] P. J. Mulders and J. Rodrigues, Phys. Rev. **D63**, 094021 (2001), hep-ph/0009343.
[19] M. Burkardt, Phys. Rev. **D69**, 091501 (2004), hep-ph/0402014.
[20] M. Anselmino, M. Boglione, U. D'Alesio, A. Kotzinian, S. Melis, F. Murgia, A. Prokudin, and C. Turk, Eur. Phys. J. **A39**, 89 (2009), 0805.2677.
[21] S. J. Brodsky, D. S. Hwang, and I. Schmidt, Nucl. Phys. **B642**, 344 (2002), hep-ph/0206259.
[22] D. Boer, P. J. Mulders, and F. Pijlman, Nucl. Phys. **B667**, 201 (2003), hep-ph/0303034.
[23] L. Adamczyk et al. (STAR), Phys. Rev. Lett. **116**, 132301 (2016), 1511.06003.
[24] M. Aghasyan et al. (COMPASS), Phys. Rev. Lett. **119**, 112002 (2017), 1704.00488.
[25] C. J. Bomhof and P. J. Mulders, JHEP **02**, 029 (2007), hep-ph/0609206.
[26] M. G. A. Buffing, A. Mukherjee, and P. J. Mulders, Phys. Rev. **D88**, 054027 (2013), 1306.5897.
[27] R. Kishore and A. Mukherjee, Phys. Rev. **D99**, 054012 (2019), 1811.07495.
[28] J.-P. Lansberg, C. Pisano, and M. Schlegel, Nucl. Phys. **B920**, 192 (2017), 1702.00305.
[29] S. Rajesh, R. Kishore, and A. Mukherjee, Phys. Rev. **D98**, 014007 (2018), 1802.10359.
[30] A. Mukherjee and S. Rajesh, Eur. Phys. J. **C77**, 854 (2017), 1609.05596.
[31] U. D'Alesio, F. Murgia, C. Pisano, and P. Taels, Phys. Rev. **D96**, 036011 (2017), 1705.04169.
[32] A. Mukherjee and S. Rajesh, Phys. Rev. **D93**, 054018 (2016), 1511.04319.
[33] A. Mukherjee and S. Rajesh, Phys. Rev. **D95**, 034039 (2017), 1611.05974.
[34] J. Matouek (COMPASS), J. Phys. Conf. Ser. **678**, 012050 (2016).
[35] U. D'Alesio, F. Murgia, C. Pisano, and P. Taels (2019), 1908.00446.

- [36] U. D'Alesio, C. Flore, and F. Murgia, Phys. Rev. **D95**, 094002 (2017), 1701.01148.
- [37] R. M. Godbole, A. Misra, A. Mukherjee, and V. S. Rawoot, Phys. Rev. **D85**, 094013 (2012), 1201.1066.
- [38] R. M. Godbole, A. Misra, A. Mukherjee, and V. S. Rawoot, Phys. Rev. **D88**, 014029 (2013), 1304.2584.
- [39] M. G. Echevarria (2019), 1907.06494.
- [40] C. E. Carlson and R. Suaya, Phys. Rev. **D14**, 3115 (1976).
- [41] E. L. Berger and D. L. Jones, Phys. Rev. **D23**, 1521 (1981).
- [42] R. Baier and R. Ruckl, Phys. Lett. **102B**, 364 (1981).
- [43] R. Baier and R. Ruckl, Nucl. Phys. **B201**, 1 (1982).
- [44] E. Braaten and S. Fleming, Phys. Rev. Lett. **74**, 3327 (1995), hep-ph/9411365.
- [45] P. L. Cho and A. K. Leibovich, Phys. Rev. **D53**, 150 (1996), hep-ph/9505329.
- [46] P. L. Cho and A. K. Leibovich, Phys. Rev. **D53**, 6203 (1996), hep-ph/9511315.
- [47] G. P. Lepage, L. Magnea, C. Nakhleh, U. Magnea, and K. Hornbostel, Phys. Rev. **D46**, 4052 (1992), hep-lat/9205007.
- [48] F. Abe et al. (CDF), Phys. Rev. Lett. **79**, 572 (1997).
- [49] D. Acosta et al. (CDF), Phys. Rev. **D71**, 032001 (2005), hep-ex/0412071.
- [50] C. Adloff et al. (H1), Eur. Phys. J. **C25**, 25 (2002), hep-ex/0205064.
- [51] F. D. Aaron et al. (H1), Eur. Phys. J. **C68**, 401 (2010), 1002.0234.
- [52] S. Chekanov et al. (ZEUS), Eur. Phys. J. **C27**, 173 (2003), hep-ex/0211011.
- [53] H. Abramowicz et al. (ZEUS), JHEP **02**, 071 (2013), 1211.6946.
- [54] S. Frixione, M. L. Mangano, P. Nason, and G. Ridolfi, Phys. Lett. **B319**, 339 (1993), hep-ph/9310350.
- [55] D. Boer, P. J. Mulders, C. Pisano, and J. Zhou, JHEP **08**, 001 (2016), 1605.07934.
- [56] A. Bacchetta, U. D'Alesio, M. Diehl, and C. A. Miller, Phys. Rev. **D70**, 117504 (2004), hep-ph/0410050.
- [57] A. Bacchetta, C. Bomhof, U. D'Alesio, P. J. Mulders, and F. Murgia, Phys. Rev. Lett. **99**, 212002 (2007), hep-ph/0703153.
- [58] J. Collins, *Foundations of perturbative QCD* (Cambridge University Press, 2013).
- [59] S. M. Aybat, J. C. Collins, J.-W. Qiu, and T. C. Rogers, Phys. Rev. **D85**, 034043 (2012), 1110.6428.
- [60] X. Ji, J.-W. Qiu, W. Vogelsang, and F. Yuan, Phys. Rev. Lett. **97**, 082002 (2006), hep-ph/0602239.
- [61] C. Kouvaris, J.-W. Qiu, W. Vogelsang, and F. Yuan, Phys. Rev. **D74**, 114013 (2006), hep-ph/0609238.
- [62] D. Boer and W. Vogelsang, Phys. Rev. **D69**, 094025 (2004), hep-ph/0312320.
- [63] F. Yuan, Phys. Rev. **D78**, 014024 (2008), 0801.4357.
- [64] K.-T. Chao, Y.-Q. Ma, H.-S. Shao, K. Wang, and Y.-J. Zhang, Phys. Rev. Lett. **108**, 242004 (2012), 1201.2675.
- [65] Y.-d. Li and L.-s. Liu, Commun. Theor. Phys. **29**, 99 (1998).
- [66] M. Butenschoen and B. A. Kniehl, Phys. Rev. Lett. **104**, 072001 (2010), 0909.2798.
- [67] P. Artoisenet, J. M. Campbell, F. Maltoni, and F. Tramontano, Phys. Rev. Lett. **102**, 142001 (2009), 0901.4352.
- [68] A. Buckley, J. Ferrando, S. Lloyd, K. Nordström, B. Page, M. Rfenacht, M. Schnherr, and G. Watt, Eur. Phys. J. **C75**, 132 (2015), 1412.7420.